JOURNAL OF SPACECRAFT AND ROCKETS
Vol. 33, No. 4, July–August 1996

Deployment of Dishes with Surface Discontinuities

G. Greschik*
University of Colorado, Boulder, Colorado 80309-0529

The transformation of doubly curved surfaces, without affecting their geometric integrity, into quasifoldable mechanisms via surface discontinuities is proposed. The potential high accuracy, simplicity, and relative freedom of design inherent in this concept are highlighted. Some mechanical characteristics of applications to parabolic dishes are discussed, and kinematic feasibility is demonstrated for a few example designs. Achievable stowage compactness is shown to be competitive with current technology. Functional and manufacturing concerns are summarized.

Nomenclature

D = deployed dish diameter, m, cm
d = stowage cylinder diameter, m, cm
E = Hook's modulus, Nm^{-2}
F = transverse force, N, of focal length, m
G = surface Gaussian curvature, m^{-2}
h = stowage cylinder height, m, cm
K = strip bending or torsional stiffness, Nm^2
l = length parameter along strip, m
M = strip bending moment or torque, Nm
m_i = shell bending in direction i, Nm/m
p = paraboloid parameter, m
r = distance from paraboloid center, m
t = plate thickness, m
z = height above paraboloid vertex, m
ϑ = stowage ratio
κ = curvature of folded strip, m^{-1}
κ_i = shell curvature in direction i, m^{-1}; $1/R_i$
ν = Poisson ratio

Introduction

THE unfoldability of doubly curved surfaces in the traditional sense of the word "fold" is at the heart of the challenge of shaped (parabolic, spherical, etc.) reflector dish deployment. No perfect answer to this challenge exists: the wealth of available deployment concepts represents but a variety of compromises between conflicting goals.

Despite the abundance of past propositions, a need for new reflector deployment concepts is sustained by the ever-evolving communication, remote sensing, and space observational needs of commercial and scientific missions. This need is further intensified by the current emphasis on simplicity, small size, and low cost against the backdrop of global economic constraints. The present paper proposes a new approach to doubly curved surface deployment to achieve a combination of some highly desirable features: 1) simplicity, 2) the theoretically perfect accuracy of the deployed surface, and 3) considerable freedom of deployment mechanism design. The proposed means to achieve these features is via the application of discontinuities (incisions) to the surface to transform it into a quasifoldable mechanism.The cost of this transformation is a potentially high sensitivity to environmental effects and a less than ideally compact stowed state for some designs.

First, a structural review of deployable antennae is given. The proposed concept is introduced next, and its application to parabolic dishes is discussed and illustrated with a few example configurations. Kinematic feasibility is demonstrated via breadboard models. The stowage efficiency of one example concept is shown to be competitive with existing technology via a hypothetical preliminary design. Instrumental to this comparison is the stowage ratio, a herein proposed measure of deployable reflector stowage efficiency, applicable independent of reflector size and structure. Finally, some functional, manufacturing, and design concerns that are the subject of ongoing research are summarized.

Received March 3, 1995; revision received Oct. 17, 1995; accepted for publication Oct. 20, 1995.

*Research Associate, Center for Space Construction, Department of Aerospace Engineering Sciences, Campus Box 429. Member AIAA.

Review of Deployable Antenna Concepts

The functional goal of accuracy and stiffness is best achieved by segmented antennae,[2,3] the surface of which consists of (semi-) rigid panels that well maintain their intended shapes[4] whereas, typically, overall assemblage accuracy is ensured by a backup structure. Segmented antennae are highly desirable for applications such as advanced communication antennae, submillimeter astronomical observatories, and microwave radiometers.[5,6] The rigidity of the solid antenna segments, however, results in a conflict between packaging efficiency and ease of deployment. Accordingly, segmented reflector deployment involves rather complex mechanisms,[3,7,8] a less than optimal compactness of the stowed state,[9] or expensive extravehicular activity.[10]

Another structural class of deployable antennas is stretched reflectors, the reflecting surface of which is stretched to shape via discrete structural components. The surface may be a wire mesh (mesh antennae[11,12]) or a continuous membrane,[13] and it is an approximation of the ideal shape, typically with planar facets[14–16] or cylindrical gores.[13,17] The members that stretch the surface to shape may involve 1) a truss,[16,18,19] 2) booms,[12,20] 3) a cable or a cable-and-catenary system,[15,16,20] and/or 4) radial ribs with[21] or without[13,17] circumferential stiffener (and surface support) rings.

Stretched reflectors have efficient stowage and can be deployed via a variety of simple[16] or complex[15,20] deployment (and surface support) systems to accommodate different deployment and functional requirements. The price of these advantages is the actual mechanical flexibility of the reflecting surface, which allows the improvement of operational accuracy only at the cost of increased support complexity.[14] Thus stretched antennae are limited to medium-to-high accuracy applications with approximately 1–40 cm wavelengths[22] (land mobile communications, direct broadcasting, Earth surface characteristic and atmospheric monitoring, deep space probes, etc.). The application of mesh reflectors to small wavelengths is also limited by the surface discontinuities.

If the reflecting surface is stretched to shape not by structural elements, but by distributed surface forces, the antenna is a membrane one. The forces may be provided via pressurization by gas or by an elastic spongy substance (although examples for nonstructural support also exist[23]). In the former case (inflatable antennae[24,25]), the deployed shape is typically stabilized by rigidization, that is, by imparting an appropriate stiffness to the surface by 1) impregnating (some of) the membrane laminae with a matrix that hardens in space[26] or 2) using initial overpressurization[27] to yield (one or more) soft metal (aluminum) layers of the membrane. The membrane concept involves a simple deployment mechanism, and it allows very compact packaging. For most current materials, however,

the inextensibility of the membrane necessary for the required accuracy is too difficult to realize without a bending stiffness that, in turn, may result in the rupturing or wrinkling of the material when stowed. Further, the shape of large membranes is sensitive to environmental effects, a problem that can be alleviated only with increased structural complexity, e.g., with internal cable elements[26] or with the application of the inflatable concept to reflector segments.[28] These problems, as well as the lack of relevant in-space experience, render current membrane antenna technology experimental.

The last class of antennae, shell reflectors, represents a transition between the segmented and the membrane concepts in that it entails a continuous reflecting surface with theoretically infinite membrane but finite bending stiffnesses, a true elastic shell. A shell reflector is thus continuous on the radiometric scale, it has a theoretical surface accuracy limited by manufacturing tolerances only, and its simple deployment may be powered by the shell's elastic straining when stowed. The price for these advantages is 1) the need for additional (such as edge) support in the deployed state and 2) an often less than ideally compact stowed state. Two reflectors of this class are the one-piece dish of Composite Optics, Inc.,[29] and the large deployable antenna furlable strip reflector.[30] When stowed, the former is rolled into a cigar-shaped bundle, whereas the latter concept involves several rolls for strips across the reflector surface that require extensive support when deployed. (The deployment concept that is the focus of the present paper[31] is concerned with one-piece shell reflectors, self-deployable from a quasifolded stowed state, as will be described.) Hybrid structures that involve more than one of the outlined four structural concepts also exist.[32]

Forming a Deployment Mechanism via Incisions

To fold, in the common sense of the word, a doubly curved surface (one with a nonzero Gaussian curvature) is impossible. If, however, a fold is interpreted not as a crease line but as a zone of intense bending (cf. the folding of a carpenter tape), folding and doubly curved surface geometry are no longer incompatible. Considering that even the rollup—the forming of a fold of indefinite length—of a helical tubular strip is possible,[33] one can conclude that practically any strip cut out of a sufficiently smooth shell is foldable, and if the latter is thin enough, the fold is elastic.

The foldability of virtually any doubly curved strip and the fact that a surface can always be subdivided into strips suggest that, at the cost of a surface subdivision, any general surface might be rendered foldable. This is apparently so for a rectangular patch (Fig. 1a) that can be subdivided into strips by slits aligned with one of the two parallel edge pairs such that the strips thus produced are left interconnected at their ends (along **AD** and **BC**, Fig. 1b). The resulting assemblage can be folded as in Fig. 1c. If the surface, as suggested in Fig. 1, has a positive Gaussian curvature, the parallel strips are uniformly oriented and, consequently, they will tend to fold uniformly. (In reality, this process would involve local stability phenomena: warping and popping. Nevertheless, the engendered perturbations do not affect the global kinematics. Accordingly, they are paid no further attention.)

One way the role of the incisions in producing a foldable mechanism can be interpreted is through the folds they themselves form: de facto hinges with (constrained) bending, torsional, and translational degrees of freedom. An alternative interpretation for their role is to relieve the membrane stresses that would develop if folding of the continuous shell was attempted. In the latter context, the proposed deployment concept is related to the application of incisions to foldable tubes to relieve stresses that would otherwise impede deployment.[34]

For a future realization of the concept via a composite shell, the generation of discontinuities will be a technological challenge. Clearly, the actual slicing of a cured laminate is unrealistic—the shell should be laid out and cured with the discontinuities in place. A reliable and affordable means for this is yet to be explored.

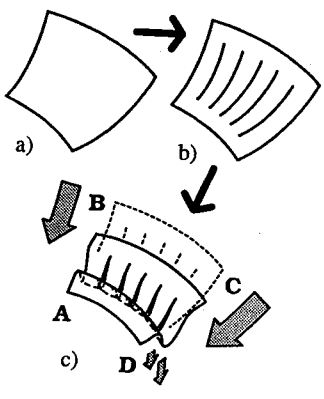

Fig. 1 Folding a rectangular surface patch.

Application to Parabolic Dishes

Loads Required to Fold a Strip

The support forces and moments needed to fold a strip (and to maintain its folds) strongly depend on the strip length. This is easily seen if the scaling of the longitudinal geometry of a folded strip with a factor α while preserving its cross section geometry (Figs. 2a and 2b) is considered. This selective scale of geometry does not change shell bending stiffness; thus, it scales the support moments and forces with factors of α^{-1} and α^{-2}, respectively:

$$M_{sc} = K\kappa_{sc} = \alpha^{-1}K\kappa = \alpha^{-1}M \tag{1}$$

for cross-section bending and torsion and

$$F_{sc} = \frac{dM_{sc}}{dl_{sc}} = \frac{d[\alpha^{-1}M]}{d[\alpha l]} = \alpha^{-2}\frac{dM}{dl} = \alpha^{-2}F \tag{2}$$

for transverse forces. The axial forces are scaled similarly, since they are, herein, intimately coupled to the former.

Another factor that affects the support loads at the ends of a folded strip is local surface geometry. Consider a surface element of Gaussian curvature G and strain-free principal curvatures κ_1 and κ_2 (with the relative magnitudes of κ_1 and κ_2 insignificant). The stretch-free bending of the element along principal direction 1 into (colinear) principal curvatures κ_1' and κ_2' (no torsion in the 1-2 reference frame) implies

$$\kappa_1\kappa_2 = \kappa_1'\kappa_2' = G \tag{3}$$

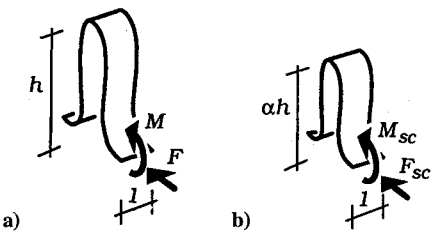

Fig. 2 Scaling of a strip's longitudinal geometry.

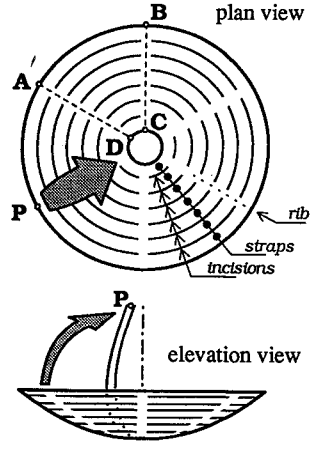

Fig. 3 Simple incision pattern.

Assuming that the shell is sufficiently thin, the vector $\boldsymbol{m}$ of shell bending moments m_1 and m_2 can be calculated via the appropriate part of the plate flexural stiffness matrix[35] $\boldsymbol{D}$ and using Eq. (3) as

$$\boldsymbol{m} = \begin{pmatrix} m_1 \\ m_2 \end{pmatrix} = \boldsymbol{D} \cdot \Delta\boldsymbol{\kappa} = D(\kappa_1' - \kappa_1) \begin{bmatrix} 1 & \nu \\ \nu & 1 \end{bmatrix} \cdot \begin{pmatrix} 1 \\ G/(\kappa_1'\kappa_1) \end{pmatrix} \tag{4}$$

in which $D = Et^3/[12(1-\nu^2)]$ is the plate flexural rigidity and the dot is the inner product.

The doubly curved geometry of the strip is reflected in Eq. (4) by the second component of the $\Delta\boldsymbol{\kappa}$ vector. For a given Gaussian curvature G, the sign of $(\kappa_1'\kappa_1)$ determines whether the geometry implies an increase or a decrease of m_1 for the $\Delta\kappa_1 = (\kappa_1' - \kappa_1)$ curvature change, that is, whether the shell is stiffened or softened against bending in the 1 direction. For a paraboloid $z = r^2/(4p) = (x^2 + y^2)/4p$, this effect is most pronounced at the center ($r = 0$), where

$$G = \kappa_{\text{cir}}\kappa_{\text{rad}} = \frac{\kappa_{\text{cir}}^2 4p^2}{4p^2 + r^2} = \frac{4p^2}{(4p^2 + r^2)^2} \tag{5}$$

is at its maximum. A paraboloid also implies $G > 0$, which means that opposite signs of κ_1' and κ_1 stiffen the fold.

Note that the realistic interaction of torsion, bending, as well as shear and axial forces in the context of a bent real strip assemblage is not reflected by the preceding simplistic derivations. Nevertheless, they suffice in highlighting some of the basic trends that affect the mechanics of such a model. These trends are well exemplified by the circumferentially repetitive direct application of the pattern of Fig. 1 to a dish, as shown in Fig. 2. One might expect that, as suggested by the figure, if the radial ribs are folded and bent upward and toward the dish axis, the sets of parallel circumferential straps between them fold outward, and a multiple version of the mechanism of Fig. 1c results. The different strap lengths and the dish geometry, however, stiffen the center of the assemblage such that the envisioned kinematics cannot be enforced by the pulling together of the rib ends.

Stress Concentrations

Another concern related to the pattern of Fig. 3 of particular relevance to composite shells, is the stress concentrations effected by the surface discontinuities via two distinct mechanisms. First, high stresses are engendered at the incision endpoints under practically any straining, as would occur in any structure with similar discontinuities. Second, the concurrent rib and strap bending results in concentrated bending across the ribs between adjacent strips (Fig. 4) because the incision pattern leaves no room for gradual rib bending.

The effects of the former mechanism may be lessened via classic techniques, such as ending the discontinuities in rounded holes. To remove the bending concentrations, on the other hand, sufficient rib lengths (weak zones) for the development of smooth bending need to be provided. Although, within the context of the pattern of Fig. 3, such weak zones can only be created with a complicated pattern of auxiliary incisions,[31] auxiliary incisions remain a viable tool to control bending for other configurations.

Practicable Incision Patterns

The excessive stiffness of the dish center with respect to the dish perimeter for the pattern of Fig. 3 can be either alleviated or exploited by design. Within the paradigm of a uniformly thick shell, the former can be achieved via radial incisions in the vicinity of the dish center, the lengths of which are not limited by the circular symmetry. Two possible such patterns are outlined in Figs. 5a and 5b with upward-folded continuous and discontinuous dish perimeters, respectively. The corresponding folding mechanisms are illustrated via plastic breadboard demonstration models of approximate deployed diameters $D = 18$ cm and focal lengths $p = 4.75$ cm in Figs. 6 and 7.

To exploit, rather than to alleviate the dish center's stiffness, a central region of the dish may be left continuous, as shown in Figs. 8a and 8b for the cases of continuous and discontinuous dish perimeters folded into the dish center. The corresponding deployment mechanisms are illustrated via models similar to those in Figs. 9 and 10. The sevenfold symmetry of the design in Fig. 8b is a result of a criterion for inward foldability that limits the angular petal dimensions

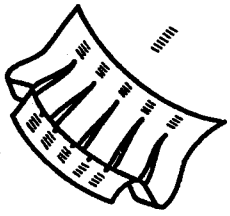

Fig. 4 Concentrated bending.

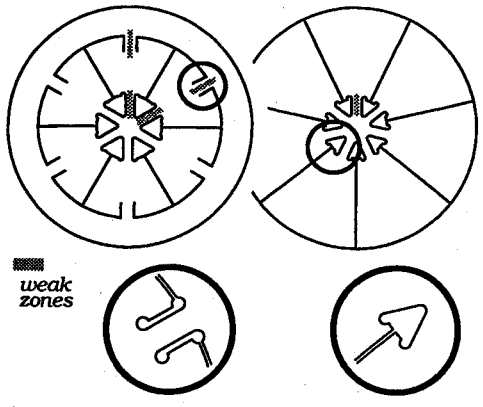

Fig. 5 Incision patterns for a flexible dish center.

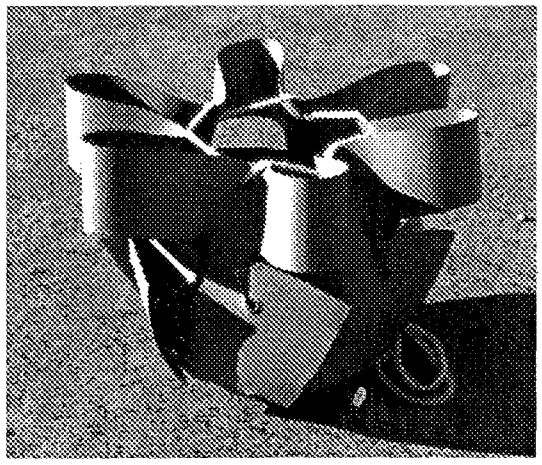

Fig. 6 Partially folded model for Fig. 5a.

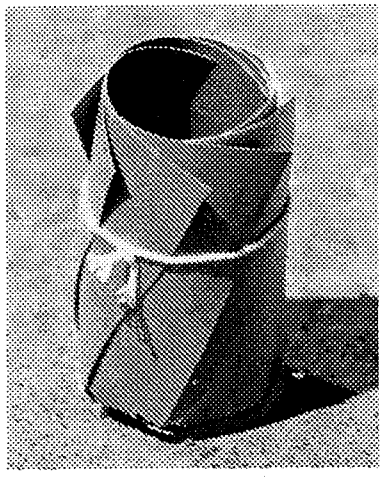

Fig. 7 Folded model for Fig. 5b.

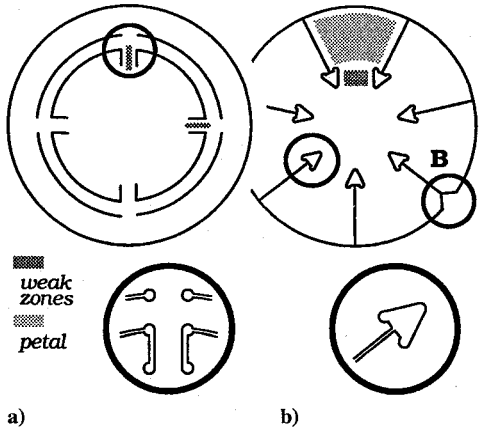

Fig. 8 Incision patterns for a stiff dish center.

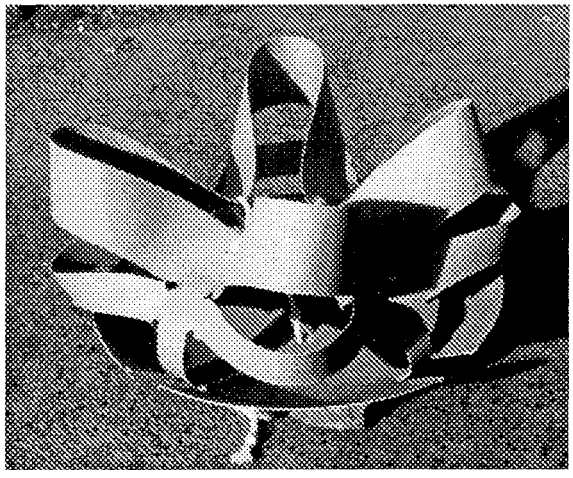

Fig. 9 Partially folded model for Fig. 8a.

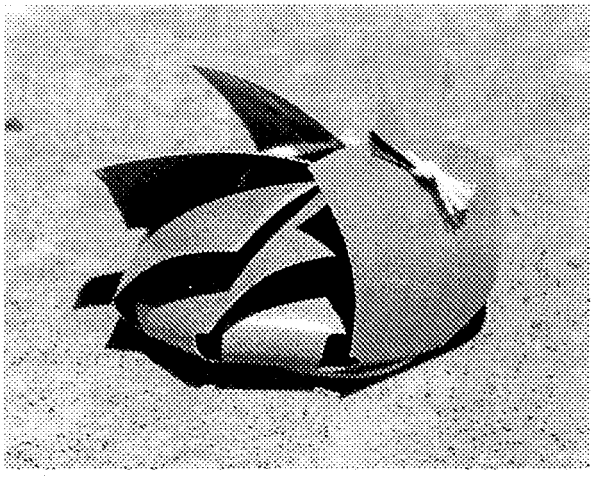

Fig. 10 Partially folded model for Fig. 8b.

to 60 deg, i.e., more than six dish segments. If permissible, the shaping of the petal corners (detail **B** in Fig. 8b) can improve stowage compactness by eliminating interference with the bent necks on the opposite side.

Stress concentrations are alleviated in the example designs by shaping the incision corners and edges, as highlighted with figure insets. The connections of the round holes at the incision ends to the neck edges (the loci of intense bending) are tangential to ensure uniformly weak cross sections along the neck lengths and, consequently, smooth bending distributions. If the hole at the incision end locally narrowed the neck, a concentration of bending would occur.

The global kinematics of the example configurations with discontinuous dish perimeters are reminiscent of some segmented concepts. In particular, the designs of Figs. 5b and 8b have petal arrangements and motions similar to the Dornier segmented antenna[2] and the single ring precision segmented reflector SCOPE,[3] respectively. The present concept, however, integrates the petals via elastic folded shell strips, rather than with hinges.

Although the deployed states of designs Figs. 5b and 8b differ only quantitatively, a striking difference in their structural performances is apparent even from a rudimentary study of the models. The deployed model of Fig. 7 is unable to maintain its shape even under its own weight, whereas that in Fig. 10 withstands some extra loads as well. Interconnecting the petal outer edges in the former case (which is equivalent to design Fig. 5a) does not improve performance beyond that of design Fig. 8b.

Apart from its apparent stiffness, design Fig. 8b also offers the further advantages of, first, a healthy petal aspect ratio and, second, a possible hybrid segmented design: rigid petals and dish center integrated via flexible shell necks. These advantages may 1) simplify design and manufacturing; 2) offer (relatively) easy means of shape control via, e.g., smart structure concepts/piezoelectric laminates at the necks; 3) enable modest structural dimensions (extending to the inner petal edges only) of a backup support if needed; and 4) permit the attachment of adjacent petal edges to one another after deployment. Further, the measured 190-cm^3 stowed volume of the model in Fig. 10 is one of the more compact ones among the stowed volumes of the other models (570, 82, and 860 cm^3 for the models of Figs. 6, 7, and 9, respectively).

Example Design

Since the advantages of the configuration of Fig. 8b just highlighted are also coupled with incision pattern simplicity, it is deemed the most desirable of those proposed. An example preliminary design of this configuration is illustrated in Fig. 11 along with the stowed state. The petals are shaped to better fit the envelope delimited by the petal necks bent in the stowed state, a dashed line for petal Q. The reflector's effective radius is thus less than the maximum radius: $R_e < R_1$. The dimensions necessary for a realistic assessment of the stowage efficiency are estimated in the following.

For compatibility with the relevant parts of Ref. 36, consider the dish with representative dimensions for multipurpose small satellite applications: a $D = 120$ in. $= 3.048$ m diam and focal length $F = D$. Let the antenna's constitutive shell be a midsurface symmetric 6-ply P75/ERL1962 laminate (of near zero coefficient of thermal expansion) with 60-deg orientation offsets between adjacent plies and a $t = 0.254$ mm total thickness.

For the rigid dish center and the petals, take a honeycomb core under a laminate face sheet yielding a 1.5-cm total thickness. Adding

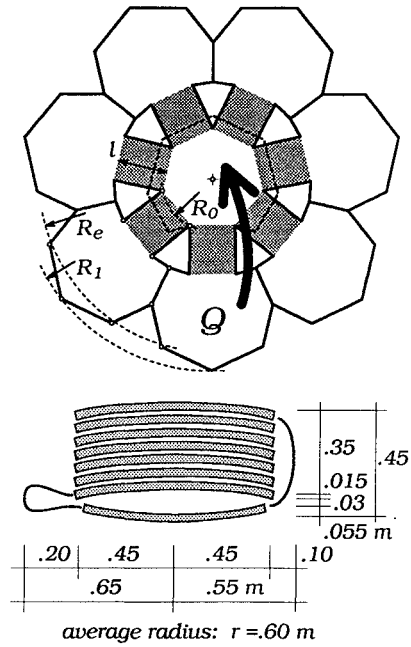

Fig. 11 Example design and schematic package cross section.

3.0 cm additional depth for stiffener ribs results a panel thickness of 4.5 cm. Padded with a 0.5-cm margin to account for differences in geometry, orientation, and misalignment of subsequently stacked petals in the stowed state, this produces a total of 5.0-cm stack thickness per panel. The stack of all seven petals, therefore, is 35 cm thick. Petal neck lengths are subsequently estimated as $l = 0.45$ m (assuming that the irregularities of the panel stack ease the arrangement of petal necks where needed).

From an expected maximum effective panel radius of 0.40 m (slightly less than the estimated maximum radius 0.45 m shown in the figure), a 1.5-cm cupping is approximated for all panels. This adds to the bottom panel thickness (of 5 cm), as well as to the 35 cm thickness of the stack of petals if the overall stowage is considered. Assuming a 3-cm gap between the dish bottom panel and the stacked petals, the total height of the package—and that of an assumed cylindrical stowage envelope—is $h \approx 0.45$ m (cf. Fig. 11).

From the assumed panel dimensions and the 45-cm neck lengths (the lateral expanse of which, when folded, is taken to extend 10–20 cm beyond the perimeter of the panels), the average cylindrical stowage radius is estimated as 60 cm (cf. Fig. 11). The resulting stowage volume is thus $V \approx 0.51$ m^3.

Note that a multiple bending of the necks in the stowed state is necessary to realize the assumed stowed dimensions, especially for the petals close to the bottom of the stack. According to the relevant results of Danley,[36] the bending of the herein assumed laminate into radii $\rho < 1.7$ in. $= 43.2$ mm engenders less than 19.5 ksi maximum ply stresses if the ply orientation deviates less than ± 5 deg from an optimal direction. This radius is sufficiently small to permit the presently assumed folding with a margin of safety deemed sufficient to account for the slight difference of the present geometry from the cylindrical and planar ones studied by Danley.[36]

Stowage Efficiency

To compare the sheer stowage efficiency inherent in deployment concepts conceived for dishes of various sizes and constructions, a dimensionless measure independent of particular mission needs (reflector shape, launch vehicle shroud, etc.) is needed. One such measure, defined herein as the stowage ratio ϑ, is the ratio of the stowage envelope's total surface to the area of the aperture plane covered by the deployed reflector:

$$\vartheta = \frac{\text{surface of stowed volume}}{\text{covered area of aperture plane}} \tag{6}$$

The lower the stowage ratio, the more efficient the stowage.

As ϑ involves the surface, rather than the volume of the stowed package, it implies a limit on the stowed volume (the volume of a sphere with the given surface) and concurrently carries a welcome bias in favor of balanced aspect ratios. Further, ϑ measures the abstract compactibility of a given mechanism regardless of size, but clearly, as a function of the relative measures of geometry (aspect ratios, etc.) within a structure. Accordingly, it eliminates scaling effects to the extent of the immunity to scaling of the relative geometry within a structure.

Table 1 shows the stowage ratios derived from assumed cylindrical stowage envelopes for some dishes, viz., the Sunflower[9] and its descendant[2] concepts (SUNF, SUNF-2), the Composite Optics one-piece shell reflector (COI),[36] the hybrid example design outlined in the preceding section (GRG), and the Dornier[2] (DORN) and the SCOPE[3] concepts, without the feed. The design proposed herein is clearly competitive with existing technology.

Table 1 Stowage ratios ϑ for some deployable dishes

Concept	D, m	d, m	h, m	ϑ
SUNF	9.6	4.4	3.5	1.10
SUNF-2	15.0	4.4	6.6	0.69
COI[a]	3.0	0.5	3.0	0.72
GRG[a]	3.0	1.2	0.45	0.6[b]
DORN	—	—	—	1.3[b,c]
SCOPE	—	—	—	0.9[b,c]

[a]Without backup support.
[b]One-digit precision signals lower accuracy.
[c]Estimated from figures.

Summary

A novel reflector dish deployment concept based on the transformation of doubly curved shells into quasifoldable mechanisms via surface discontinuities (incisions) has been proposed, and its practicability for parabolic dishes has been demonstrated via breadboard demonstration models. These examples highlighted two major advantages of the proposed concept: simplicity and a considerable freedom of deployment mechanism design.

The realization of the new concept's third major advantage, the potential for high accuracy, would depend on the dynamic characteristics of particular designs. The qualitative analysis of the demonstration models revealed significant stiffness performance variations between incision patterns. Studies of complete numerical models and/or full-size test specimens will be needed to evaluate the effects of reflector dynamics on surface accuracy for designs of interest. The models, however, suggest that the degradation of structural integrity due to the discontinuities may still permit sufficient performance for some incision patterns.

The stowed state compactness of the reviewed configurations also varied widely. However, the stowage efficiency of one of the more compact designs (the one that appeared most favorable from other practical viewpoints) has been shown to be competitive with existing technology. Instrumental to reaching this conclusion has been the herein defined dimensionless measure of stowage ratio that relates the surface of the stowage volume to the surface of the reflector's aperture plane covered in the deployed state.

Despite demonstrated aspects of the practicability and practicality of the proposed concept, a number of questions remain to be answered before a possible application. These, which are the subject of ongoing research, include 1) the dynamic characteristics of the deployed surface and the sensitivity of surface accuracy to dynamic environments; 2) design and manufacturing methodology for composite shells with discontinuities; 3) deployment control to optimize the dynamic effects of deployment on spacecraft; 4) optimal support in the stowed state and auxiliary support in the deployed state; 5) means to recover some of the structural integrity lost due to the incisions (e.g., to attach adjacent rigid petals to one another after deployment for hybrid designs); 6) effects of thermal loads; 7) active shape control; 8) the extent and effects of, as well as the optimal means to alleviate, stress concentrations; and 9) the use of piezoelectric laminates/smart structural concepts. Alternative incision patterns are also being sought.

Acknowledgments

The support of the Center for Aerospace Structures and of the Center for Space Construction of the University of Colorado at Boulder during the course of this work is gratefully acknowledged. The writer thanks Martin M. Mikulas and K.-C. Park for their inspiring cooperation and consultation.

References

[1]Anon., *Large Space Antenna Systems Technology*, NASA CP-2368, Dec. 1984.

[2]Hedgepeth, J. M., "Structures for Remotely Deployable Precision Antennas," NASA CR-182065, Jan. 1989.

[3]Mikulas, M. M., and Withnell, P. R., "Construction Concepts for Precision Segmented Reflectors," AIAA Paper 93-1461, April 1993.

[4]Manhart, P. K., and Rodgers, J. M., "Segmented Mirror Manufacturing and Alignment Tolerances (SMMAT)," NASA JPL-89-3, March 1989.

[5]Anon., "The Large Deployable Reflector (LDR) Report of the Science Coordination Group," NASA JPL-86-46, Oct. 1986.

[6]Anon., "Outlook for Space," NASA Task Group, NASA SP-386, Jan. 1976.

[7]Takamatsu, K. A., and Onoda, J., "New Deployable Truss Concepts for Large Antenna Structures or Solar Concentrators," *Journal of Spacecraft*, Vol. 28, No. 3, 1991, pp. 330–338.

[8]Hedgepeth, J. M., "Pactruss Support Structure for Precision Segmented Reflectors," NASA CR-181747, June 1989.

[9]Anon., "Sunflower Solar Collector," TRW Inc., NASA CR-46, May 1964.

[10]Mikulas, M. M., Collins, T. J., and Hedgepeth, J. M., "Preliminary Design Considerations for 10–40 Meter-Diameter Precision Truss Reflectors," *Journal of Spacecraft*, Vol. 28, No. 4, 1991, pp. 439–447.

[11]Miura, K., and Miyazaki, Y., "Concept of the Tension Truss Antenna," *AIAA Journal*, Vol. 28, No. 6, 1990, pp. 1098–1104.

[12]Anon., "Development of the 15 m Diameter Hoop Column Antenna," Harris Corp., NASA CR-4038, 1986.

[13]You, Z., and Pellegrino, S., "Dynamic Deployment of the CRTS Reflector," *Proceedings of the AIAA/ASME/ASCE/AHS/ASC 35th Structures, Structural Dynamics, and Materials Conference* (Hilton Head, SC), Pt. 3, AIAA, Washington, DC, 1994, pp. 1497–1505.

[14]Natori, M. C., Takano, T., Inoue, T., and Noda, T., "Design and Development of a Deployable Mesh Antenna for MUSES-B Spacecraft," AIAA Paper 93-1460, April 1993.

[15]Lowe, E., Josephs, M., and Hedgepeth, J., "Advanced Deployable Reflectors for Communication Satellites," AIAA Paper 93-0978, Feb. 1993.

[16]You, Z., and Pellegrino, S., "Deployable Mesh Reflector," *Spatial, Lattice, and Tension Structures*, edited by J. F. Abel, J. W. Leonard and C. U. Penalba, American Society of Civil Engineers, New York, pp. 103–112.

[17]Freeland, R. E., Garcia, N. F., and Iwamoto, H., "Wrap-rib Antenna Technology Development," *Large Space Antenna Systems Technology*, NASA CP-2368, Dec. 1984, pp. 139–166.

[18]Fager, J. A., "Status of Deployable Geo-Truss Development," *Large Space Antenna Systems Technology*, NASA CP-2269, Pt. 1, Dec. 1982, pp. 513–525.

[19]Coyner, J. V., "Box-Truss Development and Its Applications," *Large Space Antenna Systems Technology*, NASA CP-2368, Dec. 1984, pp. 213–233.

[20]Miura, K., Takano, T., Inoue, T., and Tanizawa, K., "Structural Design of a 10 m Diameter Tension Truss Antenna," International Astronautical Federation, IAF-91-316, Paris, France, Oct. 1991.

[21]Kellermeier, H., Vorbrugg, H., and Pontoppidan, K., "The MBB Unfurlable Mesh Antenna (UMA): Design and Development," *Proceedings of the Communications Satellite Systems Conference* (San Diego, CA), AIAA, New York, 1986, pp. 417–425.

[22]Roederer, A. G., and Rahmat-Sahmii, Y., "Unfurlable Satellite Antennas: A Review," *Annales des Telecommunications*, Vol. 44, No. 9, 10, 1989, pp. 475–488.

[23]Freeland, R. A., "Survey of Deployable Antenna Concepts," *Large Space Antenna Systems Technology*, edited by E. B. Lightner, Pt. 1, NASA, Nov.–Dec. 1983, pp. 381–421.

[24]Freeland, R. E., and Bilyeu, G., "In-Step Inflatable Antenna Experiment," International Astronautical Federation, IAF-92-0301, Paris, France, Aug.–Sept. 1992.

[25]Reibaldi, G., Hammer, J., Bernasconi, M. C., and Pagana, E., "Inflatable Space Rigidized Reflector Development for Land Mobile Missions," *Proceedings of the Communications Satellite Systems Conference* (San Diego, CA), AIAA, New York, 1986, pp. 533–538.

[26]Natori, M. C., Higuchi, K., Sekine, K., and Okazaki, K., "Advanced Concepts of Inflatable Rigidized Structures for Space Applications," AIAA Paper 94-1473, April 1994.

[27]Friese, G. J., Bilyeu, G. D., and Thomas, M., "Initial '80s Development of Inflated Antennas," NASA CR-182065, Jan. 1983.

[28]Natori, M., Furuya, H., Kato, S., Takesita, Y., and Sakai, T., "A Reflector Concept Using Inflatable Elements," *Proceedings of the 16th International Symposium on Space Technology and Science* (Sapporo, Japan), Publications Committee, 1988, pp. 459–467.

[29]Stumm, J. E., and Kulick, S., "Unfurlable, Continuous-Surface Reflector Concept," NASA CP-3040, Sept. 1988, pp. 129–136.

[30]Rogers, C. A., Stutzman, W. L., Campbell, T. G., and Hedgepeth, J. M., "Technology Assessment and Development of Large Deployable Antennas," *Journal of Aerospace Engineering*, Vol. 6, No. 1, 1993, pp. 34–54; also International Astronautical Federation, IAF-90-051, Oct. 1990.

[31]Greschik, G., "The Unfolding Deployment of a Shell Parabolic Reflector," AIAA Paper 95-1378, April 1995.

[32]Archer, J. S., and Palmer, W. B., "Antenna Technology for Quasat Applications," *Large Space Systems Technology*, NASA CP-2368, Dec. 1984, pp. 251–270.

[33]Greschik, G., Park, K. C., and Natori, M., "Helically Curved Unfurlable Structural Elements: Kinematic Analysis and Laboratory Demonstration," *Journal of Mechanical Design* (to be published).

[34]Jones, I. W., Boateng, C., Williams, C. D., "An Evaluation of Foldable Tubes for Application in Space Structures," *Proceedings of the 1985 SEM Spring Conference on Experimental Mechanics* (Las Vegas, NV), Society for Experimental Mechanics, Bethel, CT, 1985, pp. 590–598.

[35]Calladine, C. R., *Theory of Shell Structures*, 1st paperback ed., Cambridge Univ. Press, Cambridge, England, UK, 1988, p. 28.

[36]Danley, E. D., "Earth Observing Sensor Development for Geostat Furlable Microwave Antenna Reflector," Small Business Innovation Research 1st Phase Final Rept. NAS8-40114, NASA Marshall Space Flight Center, July 1994.

E. A. Thornton
Associate Editor